

## LYMPHOID NEOPLASIA

## Whole-genome sequencing reveals oncogenic mutations in mycosis fungoides

Laura Y. McGirt,<sup>1,2</sup> Peilin Jia,<sup>3,4</sup> Devin A. Baerenwald,<sup>2</sup> Robert J. Duszynski,<sup>5</sup> Kimberly B. Dahlman,<sup>6,7</sup> John A. Zic,<sup>2</sup> Jeffrey P. Zwerner,<sup>2</sup> Donald Hucks,<sup>6</sup> Utpal Dave,<sup>8,9</sup> Zhongming Zhao,<sup>3,4,7,10</sup> and Christine M. Eischen<sup>5</sup>

<sup>1</sup>Department of Hematology/Oncology, Levine Cancer Institute, Carolinas Medical Center, Charlotte, NC; and <sup>2</sup>Department of Medicine/Division of Dermatology, <sup>3</sup>Department of Biomedical Informatics, <sup>4</sup>Center for Quantitative Sciences, <sup>5</sup>Department of Pathology, Microbiology and Immunology, <sup>6</sup>Vanderbilt-Ingram Cancer Center, <sup>7</sup>Department of Cancer Biology, <sup>8</sup>Department of Medicine/Division of Hematology-Oncology, <sup>9</sup>Tennessee Valley Healthcare System, and <sup>10</sup>Department of Psychiatry, Vanderbilt University Medical Center, Nashville, TN

## Key Points

- High-throughput sequencing of MF revealed multiple mutations within epigenetic and cytokine pathways that may drive disease.
- Pharmacologically targeting the JAK3 pathway in MF results in cell death and may be an effective treatment of this disease.

The pathogenesis of mycosis fungoides (MF), the most common cutaneous T-cell lymphoma (CTCL), is unknown. Although genetic alterations have been identified, none are considered consistently causative in MF. To identify potential drivers of MF, we performed whole-genome sequencing of MF tumors and matched normal skin. Targeted ultra-deep sequencing of MF samples and exome sequencing of CTCL cell lines were also performed. Multiple mutations were identified that affected the same pathways, including epigenetic, cell-fate regulation, and cytokine signaling, in MF tumors and CTCL cell lines. Specifically, interleukin-2 signaling pathway mutations, including activating Janus kinase 3 (JAK3) mutations, were detected. Treatment with a JAK3 inhibitor significantly reduced CTCL cell survival. Additionally, the mutation data identified 2 other potential contributing factors to MF, ultraviolet light, and a polymorphism in the tumor suppressor p53 (TP53). Therefore, genetic alterations in specific pathways in MF were identified that may be viable, effective new targets for treatment. (*Blood*. 2015;126(4):508-519)

## Introduction

Cutaneous T-cell lymphoma (CTCL) is a skin malignancy with significant mortality in advanced disease (27% 5-year survival).<sup>1</sup> Mycosis fungoides (MF), the most common form of CTCL, classically presents as patches and plaques on the skin with disease progression leading to skin tumors, and lymph node, blood, and visceral involvement. The etiology of MF is unknown, but is thought to include chronic antigenic stimulation through viral/bacterial exposure,<sup>2,3</sup> environmental exposures,<sup>4</sup> and altered microRNA (miRNA) expression.<sup>5,6</sup>

A variety of genetic aberrations have been identified in MF. Specifically, mutations in the tumor suppressor p53 (*TP53*) were detected in 24% of tumor-stage MF, but less often in earlier-stage MF.<sup>7</sup> *TP53* mutations commonly demonstrate an UV B signature, with C-T transitions, suggesting UV-based therapy of early-stage disease may contribute to these mutations.<sup>7</sup> Loss of other tumor suppressor genes, including *CDKN2A* and *CDKN2B*,<sup>8,9</sup> and increased expression of *NAV3*, *JUNB*, and *c-MYC*, as well as hypermethylation of mismatch repair genes, are reported.<sup>9</sup> MF has not been associated with a specific translocation. However, MF can have chromosomal gains and losses, with the most common being gains within chromosome 7 and losses within chromosomes 1, 10, and 17.<sup>10-12</sup> It is unclear

whether any of the alterations reported have a role in the development of MF.

The Janus kinase (JAK)–signal transducer and activator of transcription (STAT) pathways, integral to interleukin-2 (IL-2) signaling and cellular proliferation, can be deregulated in MF and CTCL, including increased and constitutive phosphorylation of STAT3 and STAT5.<sup>13-15</sup> Activating mutations were identified in natural killer (NK)/T-cell malignancies<sup>16</sup> and adult T-cell leukemia/lymphoma (ATLL).<sup>17</sup> Additionally, an activating JAK3 mutation (A572V) was identified in 1 of 10 MF patient samples.<sup>18</sup>

High-throughput sequencing has identified novel genetic variants in many malignancies, including B- and T-cell lymphomas.<sup>19,20</sup> Because driver mutations in MF remain unidentified, we performed whole-genome sequencing (WGS) of MF tumor samples with matched normal skin controls, targeted deep sequencing of MF tumors, and exome sequencing of CTCL cell lines to identify mutations and altered pathways integral to MF development. Our results reveal mutations in cytokine and epigenetic regulation pathways that were common to MF tumors and CTCL lines, providing insight into MF. Our data significantly advance understanding into the genetic alterations in this malignancy and provide new avenues for treatment.

Submitted November 10, 2014; accepted June 3, 2015. Prepublished online as *Blood* First Edition paper, June 16, 2015; DOI 10.1182/blood-2014-11-611194.

L.Y.M. and P.J. are co-first authors.

Whole-genome sequencing data have been deposited in the NCBI Sequence Read Archive (SRA) database under accession SRP059214.

The online version of this article contains a data supplement.

The publication costs of this article were defrayed in part by page charge payment. Therefore, and solely to indicate this fact, this article is hereby marked "advertisement" in accordance with 18 USC section 1734.

© 2015 by The American Society of Hematology

## Methods

### Tissue procurement

Five patients with active tumor-stage MF underwent informed consent for participation in this study. Punch biopsies were obtained from a single MF tumor (tumor content  $\geq 80\%$ ) and from clinically uninvolved skin (detailed in supplemental Methods, see supplemental Data, available on the *Blood* Web site). For 1 patient, an additional biopsy was obtained from a separate tumor, and the tumor cells cultured (without a matrix) as previously described.<sup>21</sup> Additionally, frozen, banked skin biopsies from 25 MF patients were retrospectively identified. All samples were obtained under an institutional review board–approved protocol (IRB# 111143).

### WGS, exome, and Sanger sequencing/analysis

Genomic DNA from tissue was isolated using standard methods (details in supplemental Methods). Paired-end sequencing (PE-75) of genomic DNA from MF tumor and matched normal skin was performed (Illumina Genome Analyzer IIX). Reads were aligned to the human reference genome (hg19) using the Burrows-Wheeler Aligner (BWA),<sup>22</sup> followed by realignment and recalibration of the initial alignment using the Genome Analysis Toolkit (GATK).<sup>23</sup> Somatic variants were detected using VarScan2<sup>24</sup> and Strelka<sup>25</sup> (additional details in supplemental Methods). The detected variants by either tool were pooled for follow-up analysis. Candidate somatic variant calls were inspected using Integrated Genomics Viewer (IGV). Copy-number variations were detected by Control-FREE copy number and allelic content caller (control-FREEC).<sup>26,27</sup> The Clipping Reveals Structure (CREST) tool was used to detect gross structural variations (ie, translocations).<sup>28</sup> For validation, polymerase chain reaction (PCR) amplification of selected somatic single nucleotide variants (SNVs) and indels followed by Sanger sequencing was performed. Primer sequences are available upon request.

For exome sequencing, genomic DNA from CTCL cell lines was subjected to Exome capture (NimbleGen v3, 6Gb, Illumina HiSeq platform, PE-100). Reads were mapped as described in the previous paragraph followed by local realignment, score recalibration, and marking duplicate reads. Variants were called using the function “mpileup2cns” implemented in VarScan2 (additional details in supplemental Methods).<sup>24</sup> Variant annotations were based on ANNOVAR.<sup>29</sup>

### Targeted ultra-deep sequencing and analysis

For targeted ultra-deep sequencing for *JAK3*, *NOTCH2*, and *TP53*, the Illumina MiSeq platform was used. After samples were library-prepped and run on the MiSeq, reads were mapped to hg19 using BWA,<sup>22</sup> and realigned using GATK.<sup>23</sup> Variants were called using SAMtools and BCFtools (additional details in supplemental Methods).<sup>30</sup>

### UV signature analysis

We calculated the proportion of samples with dinucleotide mutations (dinucleotide polymorphism [DNP]) and those specifically with CC→TT mutations in MF tumors and 8 cancer types from which we previously collected somatic mutation data from large-scale next-generation sequencing projects.<sup>31</sup> We next combined the SNV data from our 5 MF samples with those from 121 melanoma patients. For each SNV, we collected its context sequence (one nucleotide 5′ and one 3′) to evaluate trinucleotide substitutions. We then applied the nonnegative matrix factorization (NMF) method to detect mutation signatures.<sup>31,32</sup>

### Cell death analysis

Equal numbers of CTCL cells were placed in 96-well plates (quadruplicate), and viability following treatment with 1 to 500 nM tofacitinib (Selleckchem) determined by MTS (3-(4,5 dimethylthiazol-2-yl)-5-(3-carboxymethoxyphenyl)-2-(4-sulfophenyl)-2H-tetrazolium) assay (Promega). For details on cell lines and calculations for survival curves, see supplemental Methods.

### Western blotting

Whole-cell protein lysates were extracted with radioimmunoprecipitation assay (RIPA) buffer 48 hours after dimethylsulfoxide (DMSO) or tofacitinib treatment,

and western blotted, as previously described.<sup>33</sup> Antibodies against phospho-JAK3 (Santa Cruz Biotechnology), JAK3 (Cell Signaling), STAT3 (Thermo Scientific), phospho-STAT5 (Cell Signaling), STAT5 (Cell Signaling), and  $\alpha$ -Tubulin (Sigma-Aldrich) were used.

## Results

### WGS of MF tumors revealed a spectrum of somatic genomic variants

To identify somatic genomic variants associated with MF, we performed WGS of tumor and matched uninvolved skin from 5 patients with tumor-stage MF (patient characteristics in Table 1). The mean depth of coverage for the WGS ranged from 32 to 44 for all samples (supplemental Table 1). WGS revealed an average of 27 602 (12 106–70 110) somatic SNVs and small insertions/deletions (indels), and an average of 102 (17–297) nonsynonymous or stop-gain exonic SNVs and indels across the 5 tumor samples (supplemental Tables 2–4). Indels in protein coding regions were infrequent (supplemental Tables 2 and 4). Using CREST analysis, 1 to 3 interchromosomal translocations were identified in tumors from patients 2, 3, and 5 (supplemental Table 5, supplemental Figure 1). Tumors in patients 1 and 4 had more translocations with 60 and 14, respectively. No translocations were similar between patients and were not further investigated.

The mutations identified were distributed without notable hotspots across the chromosomes (Figure 1A), and most mutations were novel (not known single nucleotide polymorphisms [SNPs] in dbSNP or in the 1000 Genome Project; supplemental Tables 3–4; supplemental Figures 1–2). Similar profiles of somatic mutation types were detected in the tumors, with intergenic and intronic mutations accounting for the vast majority of mutations (Figure 1B). There was variability in a small percentage of splicing and stop-gain mutations between samples. The mutation frequency in the 5 MF tumors was 5 to 26 per Mb with a mean of 12 mutations per Mb per tumor (supplemental Table 6), which is similar to the mutation frequency in lung cancers and melanoma.<sup>34</sup>

Sanger sequencing was performed on 92 SNVs and 5 indels to assess the accuracy of the WGS analysis. The SNVs and indels chosen included a random sampling and those with high oncogenic potential. We validated 90% of the alterations (supplemental Figure 3), and those that validated had a range of quality score and depth of coverage.

### UV signature in mutations from MF tumors

Because MF is a hematologic disease of the skin, we sought to determine whether the types of mutations identified by WGS were consistent with those caused by UV radiation. Evaluating all variants identified within the 5 MF tumors, transition (C-T or G-A) mutations were commonly observed, accounting for 40% to 65% of SNVs. Two tumors (patients 3 and 4) also had an increased frequency of A-G or T-C transitions (~20%; Figure 2A). An examination of the dinucleotide variations (DNP) in MF samples compared with other cancers showed MF had a very high proportion of DNPs (Figure 2B, supplemental Table 7). A hallmark of UV-induced mutations are transition mutations at dipyrimidines that are CC. Notably, CC DNPs in MF tumors were at a similar high proportion as those in melanoma, a malignancy known to have a UV component, and significantly higher than in other cancers (Figure 2B). Similar results were obtained when the number or the proportion of CC:GG to TT:AA mutations was evaluated (Figure 2B,

**Table 1. MF tumor samples subjected to WGS**

Patient	Ethnicity	Sex	Age, y	Tumor site	Normal tissue site	Pathology	Past therapy	Current therapy	TNMB	Clinical stage
1	White	Female	70	Knee	Back	Nontransformed	XRT	Bexarotene, vorinostat	T3, N0, M0, B0	IIB
2	White	Male	67	Upper arm	Abdomen	Granulomatous	NB-UVB	Bexarotene	T3, N2, M0, B0	IIB
3	White	Male	41	Forearm	Abdomen	Nontransformed	Bexarotene	NB-UVB, topical bexarotene	T3, N0, M0, B0	IIB
4	Black	Male	35	Scalp	Forearm	Large cell transformed	XRT, ECP bexarotene, romidepsin	Gemcitabine	T3, N2, M0, B2	IVA <sub>1</sub>
5	White	Female	69	Upper arm	Abdomen	Nontransformed	None	None	T3, N0, M0, B0	IIB

ECP, extracorporeal photopheresis; NB-UVB, narrow-band UV B; TNMB, tumor, node, metastasis, blood; XRT, local radiation therapy.

supplemental Figure 4). These results suggest that UV exposure may have a role in generating the abundant CC-TT mutations.

Evaluating the mutation signatures in MF and melanoma with NMF analysis,<sup>31,32</sup> we observed 4 distinct mutation signatures, including 3 consistent with UV exposure (signatures 2, 3, and 4; Figure 2C). The high bars in each signature indicate characteristic mutation types in their trinucleotide context (Figure 2C). Signature 1 is unique to MF. We next assessed the mutation profile in individual MF and melanoma tumors for each signature. The magnitude of each signature as a component of the overall mutation load in each sample shows that the UV-related signatures are a factor in all 5 MF samples (Figure 2D). Specifically, for signature 2, MF tumors from patients 1 and 5 showed high coefficients, indicating that this UV-related signature significantly contributes to their mutation profiles (Figure 2D). There were moderate coefficients for patients 1 and 4 for signature 3 and patients 2 to 4 for signature 4. Although these analyses may be limited by sample number, the data suggest UV may be contributing to MF.

### Mutations identified in common pathways

In the subset of genes containing exonic mutations, those likely to have a role in oncogenesis were identified. Pathway analysis of the nonsynonymous, exonic SNVs and indels revealed a diverse set of biological processes affected (Figure 3A).<sup>35</sup> Within the 5 patients, there were 42 genes implicated in other malignancies, through gain of function (oncogenes), loss of function (tumor suppressor), or aberrant expression (Figure 3B). Of note, 41% of these mutations were C to T transitions, further supporting a role for UV in MF. Five of the 42 genes had mutations in 2 of the MF tumor samples: *NCOR1*, *FAT3*, *CLUAP1*, *BAI3*, and *ZEB1* (Figure 3B and supplemental Tables 3, 4, and 8). Additionally, 10 other genes not previously linked to cancer or that have uncharacterized roles in cancer had exonic, nonsynonymous mutations in >1 tumor sample (supplemental Table 8).

To investigate similarities between tumor MF and cultured CTCL lines at the genome level, we subjected 3 CTCL cell lines (HH, Hut-78, and MyLa) to exome sequencing. We also evaluated the Cancer Cell Line Encyclopedia (CCLE), which has sequenced a panel of ~1600 genes across cell lines, including HH and Hut-78.<sup>36</sup> Eight genes with exonic mutations in 2 or more cell lines that were likely to have a role in oncogenesis were identified (Figure 3C). Among them, 1 gene was determined to have an identical mutation observed in at least 2 of the cell lines. Six of the genes that were mutated in at least 2 of the cell lines were also reported in HH and/or Hut-78 in the CCLE (Figure 3C).

Given the poorly understood therapeutic success of histone deacetylase inhibition in patients with CTCL,<sup>37</sup> the genes involved in epigenetic regulation were of specific interest. Four of five patient tumors sequenced and all CTCL lines had mutations in genes integral to

chromatin remodeling and histone modification. Mutations were identified in genes that mediate histone methylation, acetylation, ubiquitination, and chromatin remodeling (Figure 3D). Evaluation of the 10 genes mutated in patient tumors showed that they were significantly enriched compared with 24 349 known protein-coding genes in NCBI RefSeq ( $P = 2.565 \times 10^{-11}$ , Fisher exact test). Notably, mutation of *NCOR1*, a corepressor that recruits histone deacetylases to chromatin, was present in a third of the samples (2 patients and 1 cell line).

Because Th2-skewed cytokine expression has a role in MF,<sup>38</sup> we assessed genes that regulate cytokine expression or cytokine signal transduction. We identified mutations within cytokine pathway genes, and specifically in the IL-2 signaling pathway, in all but 1 of the MF tumor samples (Figure 3E). Mutations in the IL-2R signaling proteins (JAK3 kinase and its downstream target STAT5), as well as proteins that regulate IL-2 and IL-2R expression were present. Evaluation of the 4 genes mutated in patient samples showed that they were significantly enriched compared with 24 349 known protein-coding genes in NCBI RefSeq ( $P = 8.684 \times 10^{-11}$ , Fisher exact test). We also identified mutations in cytokine signaling pathway genes in the HH and Hut-78 cell lines (Figure 3E).

### SCNAs in MF

Somatic copy-number alterations (SCNAs) were assessed in each patient. We observed both broad copy-number events that span a chromosome arm or an entire chromosome and focal copy-number events that affect much smaller regions than a chromosome arm (Figure 4A). Broad SCNAs were observed in all patients except patient 5, with patient 1 displaying the highest number of such events. For example, the MF tumor in patient 1 had only 1 copy of chromosome 3 and 13, copy-number loss of 6q, 10p, and 21q, and copy-number gain of 7q and 16p. In patient 4, we observed copy-number loss in 6q and a large region spanning both arms of chromosome 13, and copy-number gain in 10p. Focal copy-number events were detected in all patients, with patient 5 displaying the most aberrant events. There were no arm-level copy-number changes in patient 5. Investigation of the focal SCNA events revealed all tumors had expected copy losses in T-cell receptor regions ( $\alpha$ ,  $\beta$ ,  $\gamma$ ) that undergo VDJ rearrangement (Figure 4B, supplemental Figure 5). These data suggest selection of a T-cell clone in each patient, supporting the clonal nature of this disease. It was also noted that the same 2 patients (1 and 4) with exonic mutations within *ZEB1* (inhibitor of IL-2 transcription<sup>39</sup>) also had loss of 1 copy of *ZEB1*, raising the possibility of *ZEB1* loss of heterozygosity being associated with the development or progression of MF. Additionally, we identified copy-number gains of both *NOTCH2* and *NOTCH2NL* across all 5 patients in both their

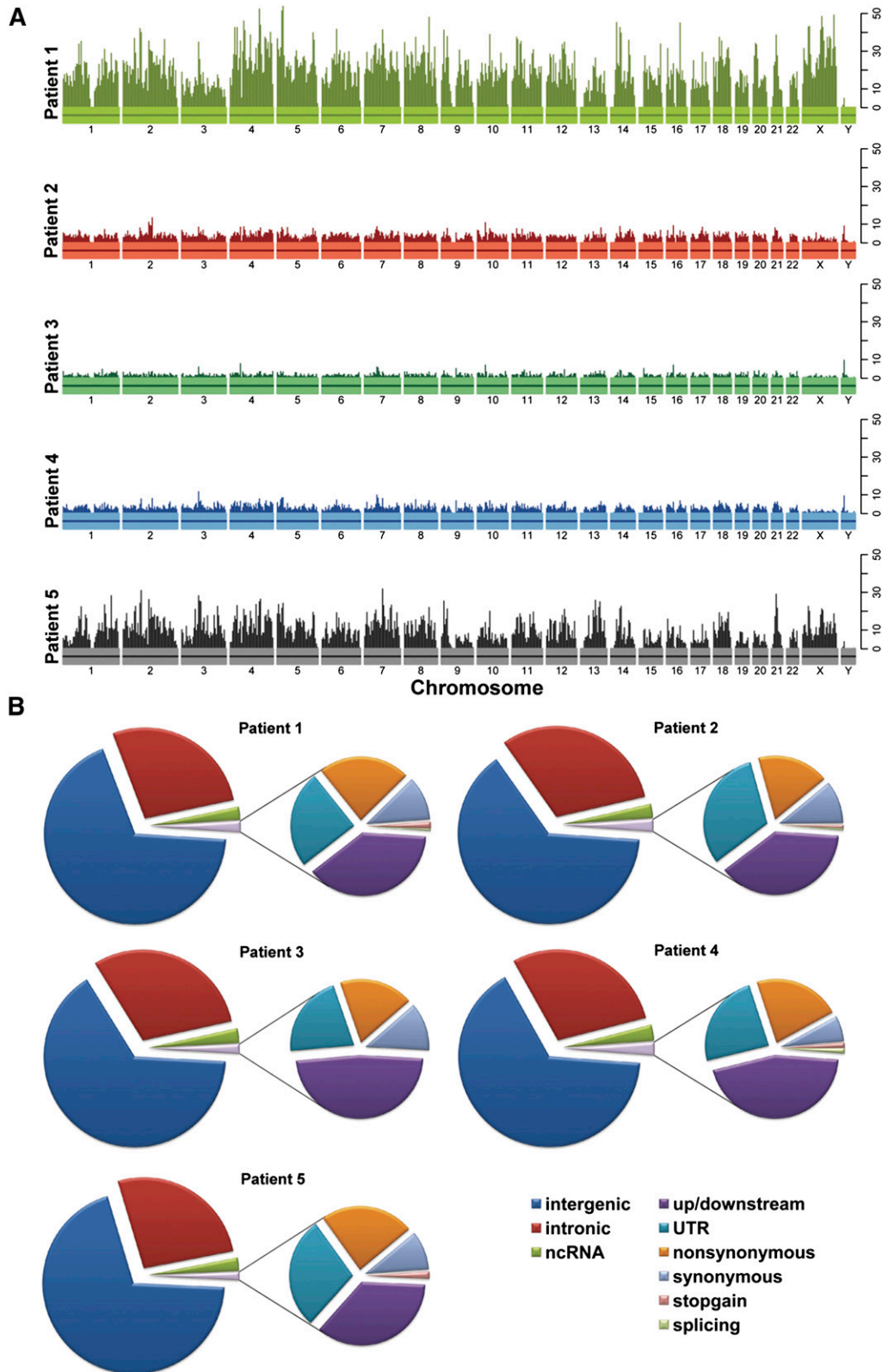


**Figure 1. Mutation profiles of patient tumors subjected to WGS.** (A) Each patient is plotted with a unique color. The vertical bars indicate the number of predicted, somatic SNVs in a 5-Mb window. (B) Pie charts of functional categories of the predicted somatic SNVs. For each patient, the left pie chart depicts the proportion of somatic mutations in categories based on their genomic location, including intergenic, intronic, ncRNA, and exonic SNVs. The right chart shows the breakdown of different mutation types in coding regions, including upstream/downstream, UTR, nonsynonymous, synonymous, stop-gain SNVs, and SNVs located in splicing sites. Only SNVs not included in dbSNP (build 131) or the 1000 Genome Project (November 2010) are shown. ncRNA, noncoding RNA; UTR, untranslated region.

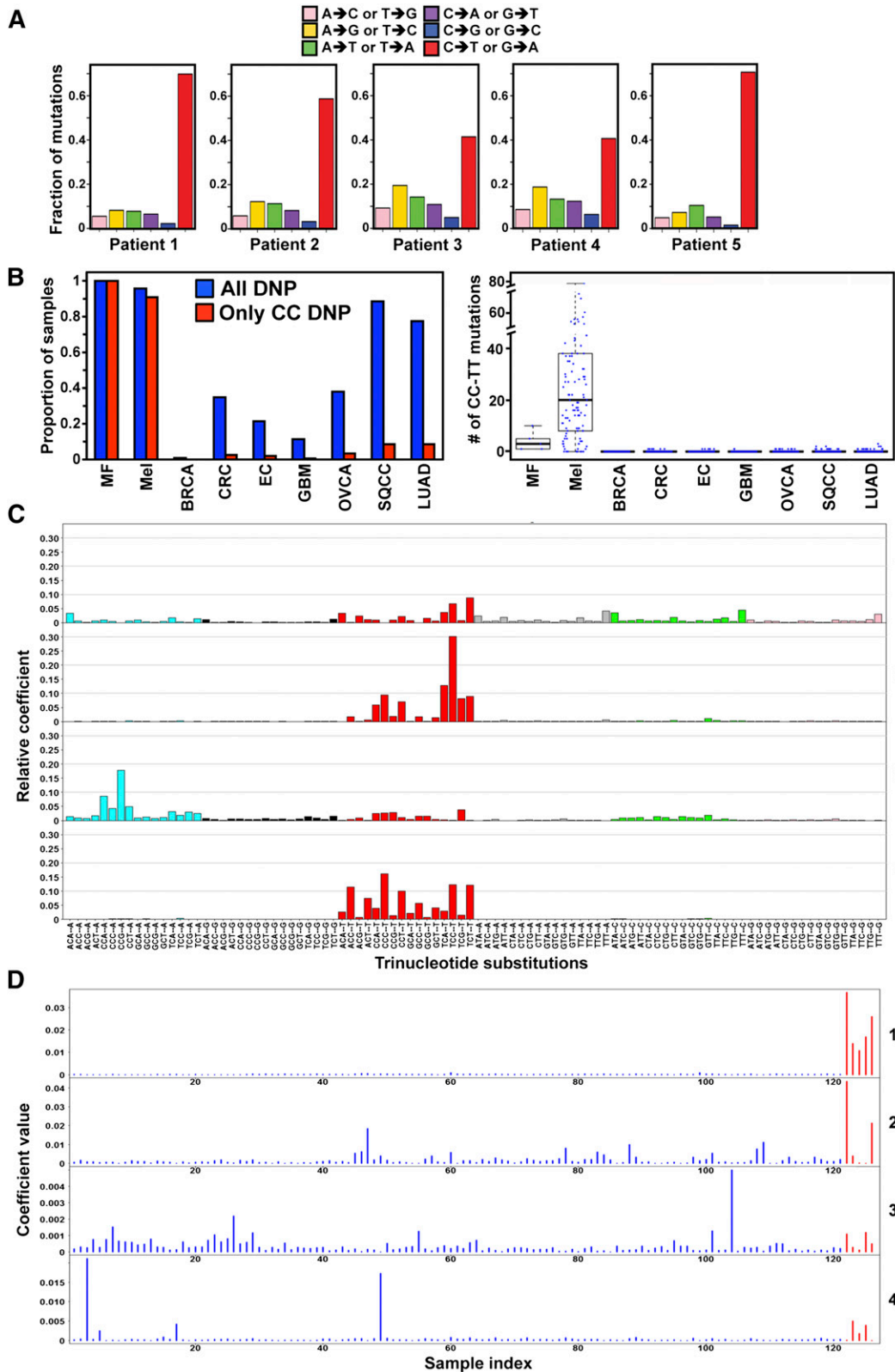
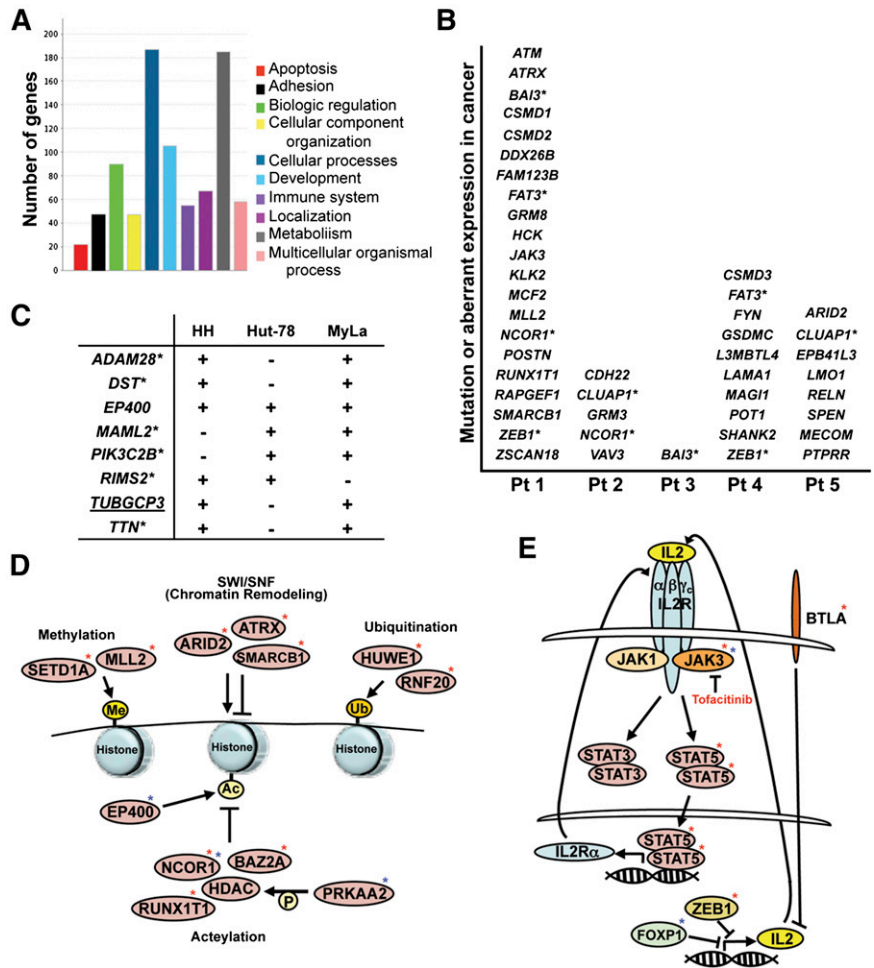


**Figure 2. Mutations in MF appear to have a UV signature.** (A) Frequency of different mutation classes in each MF patient. (B) Samples with any DNP and with mutations that specifically change CC in different cancer types (left). The number of CC:GG to TT:AA mutations in the coding regions of each cancer type (right). BRCA: breast cancer, n = 507; CRC: colon and rectal cancer, n = 224; EC: endometrial carcinoma, n = 248; GBM: glioblastoma, n = 290; LUAD: lung adenocarcinoma, n = 182; Mel: melanoma, n = 121; OVCA: ovarian carcinoma, n = 316; SQCC: squamous cell lung cancer, n = 177. (C) Four mutation signatures of MF and melanoma tumors. Each color denotes 1 of the 6 possible trinucleotide mutations. The y-axis denotes the relative coefficient of each substitution to the corresponding signature. (D) Coefficient of each MF (red) and melanoma (blue) tumor for each signature. The sample index for melanoma is x = 1:121 and MF is x = 122:126. A higher coefficient indicates a higher contribution of the corresponding signature in the sample. Only SNVs not in dbSNP (build 131) or the 1000 Genome Project (November 2010) were included.

**Figure 3. Specific mutations and the pathways affected.** (A) The number of genes in defined biological pathways with mutations in MF. (B) Genes known to have a role in cancer that were identified as mutated in MF tumor patient (Pt) samples. Genes with an asterisk denote that 2 patients had mutated that gene. (C) Genes known to have a role in cancer that were identified as mutated (+) in 2 or more CTCL cell lines. Underlined genes indicate the mutation is identical between cell lines. Genes with asterisks indicate the mutation is identical in the CCLC. (D) Mutations in genes that function in epigenetic modification and chromatin remodeling were identified in patient samples (red asterisk) and cell lines (blue asterisk). Ac, acetylation; Me, methylation; P, phosphorylation; Ub, ubiquitination. (E) Mutations in genes that function in the IL-2 cytokine pathway were identified in patient samples (red asterisk) and cell lines (blue asterisk).



normal and tumor sample, indicating these gains were germline in origin (Figure 4C).

**TP53 genetic variation is associated with MF**

A quarter of tumor-stage MF have somatic *TP53* mutations, whereas *TP53* mutations are less common in earlier disease.<sup>40</sup> Somatic *TP53* mutations were not detected in any of the 5 MF tumors evaluated by WGS. Specific polymorphisms within *TP53* are associated with susceptibility to malignancy, including *TP53* Pro72Arg.<sup>41</sup> Given its potential significance in MF,<sup>7</sup> we also evaluated *TP53* polymorphisms. In addition to the initial 5 tumor-stage patients, we also obtained banked tumor tissue from 25 patients with MF. Of the 30 MF samples, 8 (27%) were homozygous Pro/Pro, 6 (20%) were heterozygous Arg/Pro, and 16 (53%) were homozygous Arg/Arg (Table 2). There were 4 samples from black patients (13%) and 26 from white patients. Comparing our results to a published control white population (n = 335),<sup>42</sup> there was a significant increase in the frequency of Pro/Pro in our MF patients (27% vs 6%,  $\chi^2$  test,  $P < .001$ ) and a similar frequency of Arg/Arg (53% vs 58%,  $\chi^2$  test,  $P = .45$ ). When comparing only our white patients (n = 26) to the control white population, as there are ethnic differences in allele frequency,<sup>43</sup> we still obtained an increased frequency of Pro/Pro (19% vs 6%,  $\chi^2$  test,  $P = .01$ ). Fourteen of the 30 MF patients (47%) had at least 1 Pro allele, and the overall Pro allele frequency was increased compared with control (33% vs 24%,  $\chi^2$  test,  $P = .03$ ). These data suggest the proline residue may be contributing to susceptibility of MF.

**Alteration of Notch pathway in MF**

The Notch protein family consists of 4 transmembrane receptors and 5 ligands that are integral to embryogenesis and cell-fate decisions.<sup>44,45</sup> Activating mutations in *NOTCH2* were implicated in the development of both B-cell lymphomas and murine T-cell leukemia.<sup>45-47</sup> In addition to the increased copy numbers of *NOTCH2* and *NOTCH2NL* in all patients subjected to WGS (Figure 4C), we also identified other mutations affecting the Notch pathway. For example, we identified with targeted ultra-deep sequencing a patient with early plaque-stage MF who had a *NOTCH2* nonsynonymous SNV (C4699T, R1567W), which is predicted to be deleterious, and is located in the negative regulatory region between 2 previously identified gain-of-function mutations found in marginal zone lymphomas.<sup>46</sup>

**Identification of *JAK3*-activating mutations in MF**

*JAK3*-, A572V-, and A573V-activating mutations (within the pseudo-kinase regulatory domain) were reported in NK-/T-cell lymphomas (Figure 5A). The FERM domain also harbors activating mutations (L156P, R172Q, E183G) in ATLL.<sup>17</sup> We identified an activating *JAK3* point mutation in 1 of the 5 MF tumor samples by WGS (c.C1718T, p.A573V) with a variant allele frequency of 41.67%. Sanger sequencing validated the mutation and showed mutation of a single allele at the 1718 position (Figure 5B). A biopsy of a separate tumor from the same patient placed in short-term culture showed the identical *JAK3* mutation (Figure 5B). Sanger sequencing of *JAK3* in 3 CTCL cell lines revealed

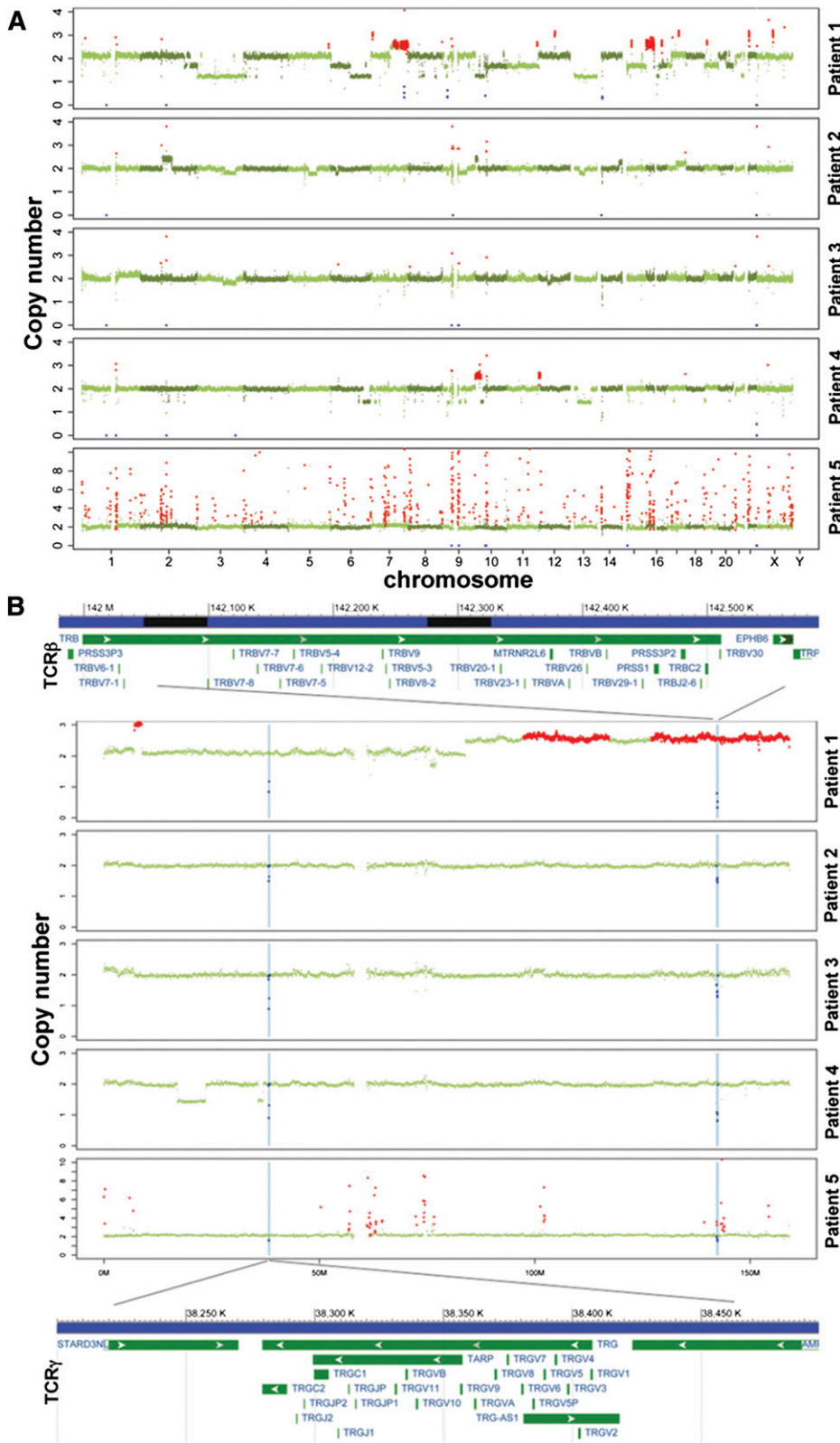


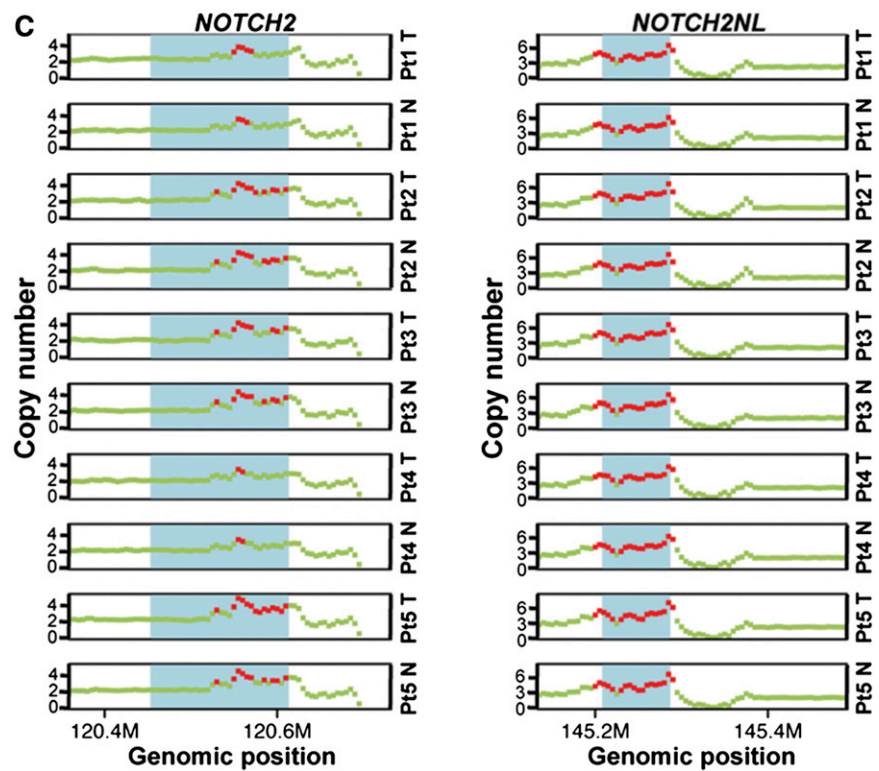
**Figure 4. Copy-number alterations in MF tumor genomes.** (A) FREEC detection of SCNAs in each patient. X-axis: genomic positions, ordered by chromosomes. Y-axis, copy numbers in tumor compared with the matched normal sample. A copy number of 2 indicates copy number neutral; red: gains, blue: losses, green: no change. (B) Deletion regions on chromosome 7 that involve T-cell receptor genes (annotations are based on human reference GRCh37/hg19); TRB: T-cell receptor  $\beta$  locus. TRG: T-cell receptor  $\gamma$  locus. (C) Amplification at the *NOTCH2* and *NOTCH2NL* loci in normal (N) and tumor (T) of each patient (Pt). Red dots: copy number  $\geq 3$ . The blue shade shows the respective gene region: *NOTCH2* (chr1:120454176-120612317) and *NOTCH2NL* (chr1: 145209111-145285912) based on UCSC Genome Browser hg19. A copy number of 2 is neutral.

the same *JAK3* C1718T (A573V) activating mutation in the Hut-78 cells (Figure 5C). *JAK3* was not mutated in HH or MyLa cells. These data suggest this *JAK3* mutation may be a contributing factor to MF.

To assess the rate of *JAK3* mutation in a larger MF population, we performed targeted ultra-deep sequencing on 25 MF samples, 17 of

which were early stage (stage Ia-IIa). Although we did not detect overt evidence of *JAK3* mutations in these samples, 5 of them had ~1% allele frequency of previously reported activating *JAK3* mutations (L156P, E183G, A572V, and A573V). Given the very low frequency of these variations and limited DNA remaining, these data could not be validated

Figure 4. (continued)



by other sequencing methods. Of note, early-stage MF have a low tumor burden and are inherently heterogeneous (mixture of cell types).

#### CTCL cells are sensitive to a JAK3 inhibitor

A JAK3 inhibitor, tofacitinib, has recently been US Food and Drug Administration (FDA) approved for rheumatoid arthritis treatment, as it inhibits the proliferation of activated T cells.<sup>48</sup> Given our results demonstrating the presence of activating *JAK3* mutations in MF and the Hut-78 line, we postulated tofacitinib may be useful as a therapeutic agent in MF/CTCL (Figure 3E). Evaluation of the JAK3/STAT5 signaling pathway in 3 CTCL lines showed increased phospho-STAT5 in Hut-78, compared with HH cells (Figure 5D). MyLa cells had robust levels of phospho-STAT5 likely due to increased STAT5 protein levels (Figure 5D). Following exposure to 200 nM tofacitinib, there were significantly reduced cell numbers for all 3 CTCL lines (Figure 5E). Notably, treatment of the CTCL lines with increasing concentrations of tofacitinib (1-500 nM) revealed a significantly reduced half-maximal inhibitory concentration ( $IC_{50}$ ) in Hut-78 compared with HH and MyLa cells (2-way analysis of variance [ANOVA],  $P < .001$ ; Figure 5F). All 3 lines had an  $IC_{50}$  well below the tofacitinib concentrations achieved in humans (85-107 ng/mL) based on FDA-approved dosage.<sup>49</sup> There was a dramatic reduction of phospho-STAT5 in both Hut-78 and MyLa cells at tofacitinib concentrations as low as 10 nM (Figure 5G). Therefore, JAK3 inhibition may be therapeutically useful for treating CTCL with activating mutations in *JAK3* as well as those malignancies with an overactive JAK3/STAT5 signaling pathway.

## Discussion

As the pathogenesis of MF is poorly understood, and previous focused genetic studies have failed to identify mutations common to MF

tumors,<sup>7-9</sup> we performed WGS of MF tumors. Our analysis revealed a wide breadth of mutations with overlap between tumors, and many of the mutations in shared biologic pathways. We identified mutations in known oncogenes and tumor suppressor genes as well as genes not previously linked to cancer and certainly not to MF.

Of note, we identified mutations in many genes involved in epigenetic regulation (Figure 3D). Of the genes mutated, 3 of them have a specific role in the methylation of H3K4, which is associated with open chromatin and active transcription.<sup>50</sup> *MLL2* is a tumor suppressor and histone methyltransferase that helps to methylate H3K4.<sup>51</sup> *MLL2* mutations were identified in B-cell lymphomas, and our novel mutation (C8788T, P2930S) is in a similar region as several previously identified.<sup>52</sup> *SETD1A*, a component of a histone methyltransferase complex that can mono-, di-, or trimethylate H3K4,<sup>53</sup> had a missense mutation in 1 MF tumor. *RNF20*, an E3 ubiquitin ligase that ubiquitinates histone 2B, which is a prerequisite for methylation of H3K4<sup>54,55</sup> had a mutation in a coiled region in 1 tumor. Our results are interesting given the successful treatment of some MF patients with histone deacetylase inhibitors (HDACi), which have been shown to stimulate methylation of H3K4.<sup>50</sup> We hypothesize mutations in the genes that regulate H3K4 methylation lead to reduced methylation, closed chromatin, and reduced transcription of tumor suppressors, which can be reversed with HDACi. These will be important areas in the future on which to focus research efforts.

Specific *TP53* polymorphisms are linked to many malignancies,<sup>56</sup> and we determined that the Pro72Arg polymorphism may be associated with MF. The proline allele is linked with improved DNA repair and cell cycle arrest, whereas the arginine allele is associated with enhanced apoptosis.<sup>57</sup> Within dbSNP the G nucleotide (Arg) is the minor allele, as we indicated; however, both proline and arginine alleles are reported as the minor allele, and ethnicity can influence allele variance.<sup>43</sup> Although a previous MF study did not find an increased frequency of Pro/Pro ( $n = 24$ ;



**Table 2. rs1042522 polymorphism in MF samples**

Sex	Ethnicity	Clinical stage	TP53 P72R
Male*	Black	IVA	CC
Female	Black	I	CC
Male	Black	I	CC
Female	White	I	CC
Female	White	I	CC
Male	White	I	CC
Female	White	IIB	CC
Female	White	IIB	CC
Female	White	I	CG
Female	White	I	CG
Female	White	I	CG
Male	White	I	CG
Female*	White	IIB	CG
Female	White	IIB	CG
Male*	White	IIB	GG
Male*	White	IIB	GG
Female*	White	IIB	GG
Male	Black	I	GG
Female	White	I	GG
Female	White	I	GG
Female	White	I	GG
Female	White	I	GG
Male	White	I	GG
Male	White	I	GG
Male	White	I	GG
Male	White	I	GG
Male	White	IIB	GG
Male	White	IIB	GG
Male	White	IVA	GG
Male	White	IVA	GG
Male	White	IVA	GG

\*Samples subjected to WGS.

European population), it demonstrated a 29% proline allele frequency in MF vs 19% in controls.<sup>57</sup> Within our cohort (30 patients), there was a significant increase of both the Pro/Pro genotype and the presence of at least 1 proline allele. Although this is a limited cohort, this *TP53* polymorphism may be associated with susceptibility to MF, and suggest that a population-based study would be beneficial.

Notch signaling is involved in a multiple cellular processes, including embryogenesis and cell-fate decisions, including lymphocyte differentiation.<sup>44,45</sup> Interestingly, *NOTCH2* mutations, gain of function, copy-number gains, and loss of function have been associated with B-cell lymphomas and chronic myelomonocytic leukemia.<sup>46,58,59</sup> We demonstrated germline copy-number gain of both *NOTCH2* and *NOTCH2NL* across all 5 MF tumors, and also identified a *NOTCH2* mutation in the negative regulatory region in a separate MF case. Germline copy-number variations can predispose to familial and sporadic cancers,<sup>60,61</sup> and we hypothesize that the increased expression of *NOTCH2* may increase susceptibility of MF/CTCL. Activating *NOTCH1* mutations frequently occur in T-cell acute lymphoblastic leukemia (T-ALL) and ATLL,<sup>62,63</sup> and a previous study identified increased *NOTCH1* expression in CTCL where treatment with a pan-Notch inhibitor led to CTCL cell apoptosis.<sup>64</sup> We propose that there may be multiple mechanisms of *NOTCH* pathway dysregulation in MF, and further consideration should be given to therapeutically targeting this pathway.

We also identified multiple mutations within the *IL-2* cytokine pathway. *ZEB1*, known to inhibit transcription of *IL-2*,<sup>39</sup> was mutated in 2 MF tumors. Although increased *ZEB1* is associated with epithelial to mesenchymal transition in cancers,<sup>65</sup> inactivating

mutations were identified in ATLL.<sup>66</sup> Similar to a mutation in ATLL, the frameshift deletion in *ZEB1* was in the *N-terminal* zinc finger repeats, and the SNV was in the C-terminal zinc finger repeats. Notably, these same 2 MF tumors had a loss of the other allele of *ZEB1*. These *ZEB1* alterations are expected to lead to a lack of inhibition of *IL-2* transcription, resulting in increased *IL-2* production and MF tumor cell growth (Figure 3E). Therefore, *ZEB1* mutation and loss of heterozygosity (LOH) may be an important contributor to MF.

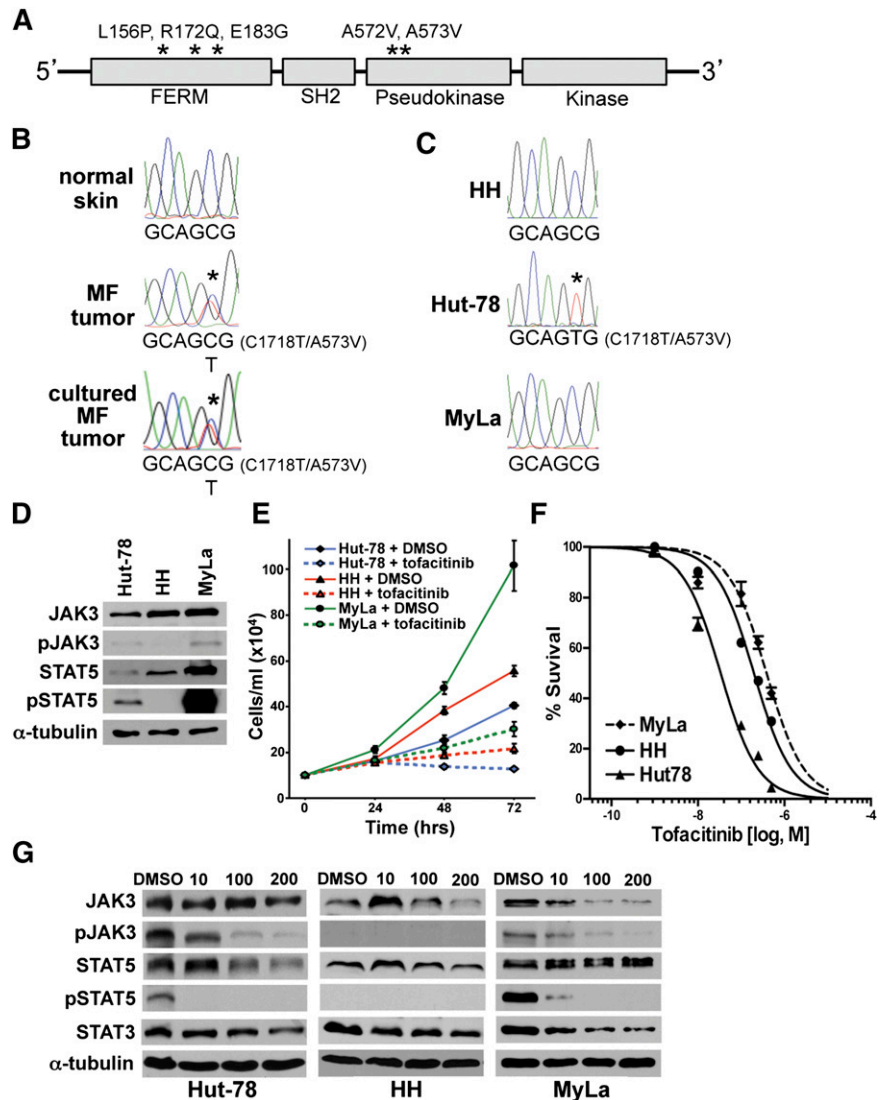
*JAK3*, which participates in transducing the *IL-2* proliferative signal through phosphorylation of *STAT* proteins (Figure 3E), has activating mutations in NK-/T-cell lymphoma (35%), ATLL (11%), and a single MF tumor.<sup>14,16-18</sup> In the current study, we identified the same activating *JAK3* mutation in an MF tumor evaluated with WGS and a CTCL line. Ultra-deep sequencing of an additional 25 MF samples revealed very low allele frequencies of known activating *JAK3* mutations in 5 samples that we were unable to validate. Thus, although interesting, these data should be taken with caution. It is possible that the heterogeneous (mixture of cell types) nature of the biopsies of patch- and plaque-stage MF and the low tumor burden of these samples (~10% in patch stage) may be masking the true incidence of *JAK3* mutation, but it is also possible that this frequency is within the margin of error or indicates a subpopulation. These findings highlight the difficulty of assessing tumor genetics in low tumor burden, heterogeneous samples. Regardless, an activating *JAK3* mutation was verified in 1 of 12 (8.3%) MF tumor-stage samples and in 1 of 3 CTCL cell lines. These results indicate *JAK3*-activating mutations may be a driver of a portion of MF.

Importantly, we determined that our CTCL cell lines were sensitive to treatment with *JAK3* inhibition. Hut-78, which harbored the activating *JAK3* mutation, was the most sensitive to tofacitinib. Although there were no *JAK3* mutations in HH or MyLa cells, they still demonstrated sensitivity to *JAK3* inhibition, indicating that they are dependent on the pathway for their growth/survival. In support of this idea, MyLa cells had increased levels of *STAT5* phosphorylation and *JAK3* autophosphorylation, both of which were inhibited by tofacitinib. HH cells did not have phospho-*STAT5* and may depend upon other downstream *JAK3* substrates such as the *AKT* pathway.<sup>17</sup> Given the advent of *JAK3* inhibitors and the sensitivity of CTCL lines, we believe it is important to consider treatment of MF with these FDA-approved medications.<sup>48</sup>

An interesting finding from our WGS analysis was that there appears to be a link between UV exposure and tumor-stage MF. There was a high frequency of UV-induced DNP mutations and mutation signatures consistent with UV exposure in all 5 MF tumors, which is comparable to melanoma, a malignancy with a known UV component. Only 2 of the 5 patients had UV therapy, but the sun exposure history for all the patients is unknown. It was proposed previously that UV exposure of MF may hasten progressive disease with UV signature *TP53* mutations in advanced disease.<sup>7</sup> It is concerning that although often effective, UV treatment of early-stage MF may create mutations leading to advanced disease, as well as increase risk of secondary skin cancer.<sup>67</sup> Although this is not unique to MF, as secondary malignancies are correlated with other cancer therapies,<sup>68</sup> our data again raise the possibility that UV exposure, including phototherapy, may contribute to MF.

Both WGS and targeted ultra-deep sequencing of specific genes are useful tools to help better detect mutations within specific genes and pathways in malignancies, as we discovered in MF. We identified genes in specific cytokine signaling pathways, cell-fate pathways, and epigenetic regulatory processes mutated in MF,

**Figure 5. Activating JAK3 mutation identified in MF tumor and CTCL cell line.** (A) JAK3 schematic with functional domains denoted. Activating JAK3 mutations previously reported and identified in this study marked with asterisks. (B) Chromatographs of Sanger sequencing of normal and tumor DNA from patient 1. The C1718T transition is detected in the tumor sample only. (C) Sequencing of CTCL cell lines showing the C1718T transition in Hut-78 cells. (D) western blots of JAK3 and proteins in its downstream pathway in CTCL cell lines; phosphorylated JAK3 (pJAK3) phosphorylated STAT5 (pSTAT5). (E) Viable cell numbers of CTCL cell lines at intervals following addition of 200 nM tofacitinib. (F-G) CTCL cell lines subjected to MTS assay (tofacitinib 1, 10, 100, 250, and 500 nM) (F) and western blot (tofacitinib 10, 100, 200 nM) (G) after 48 hours of treatment.



and a possible link to UV exposure, resulting in a better understanding of the pathogenesis of this disease. Consequently, new therapeutic options for MF have been identified and others can be developed.

the Vanderbilt Cutaneous Lymphoma Fund, an anonymous donor, and National Cancer Institute (NCI) Cancer Center Support Grant P30CA068485 utilizing the Vanderbilt Technologies for Advanced Genomics (VANTAGE) core.

### Acknowledgments

The authors thank the members of the Eischen laboratory for helpful discussions and critique, and Dr William Pao and Katie Hutchinson for assistance with MiSeq sequencing.

This work was supported in part by the Vanderbilt Ingram Cancer Center and Personalized Cancer Medicine Initiative, the Dermatology Foundation Physician-Scientist Career Development Award (L.Y.M.), the National Institutes of Health (NIH)-supported Vanderbilt Clinical Oncology Research Career Development Program (K12CA090625), Hematology Helping Hands Fund (C.M.E. and L.Y.M.), R01CA148950 (C.M.E.), the Vanderbilt University Medical Center Department of Medicine/Dermatology, the TJ Martell Foundation (K.B.D. and D.H.), the McDaniel Gift Fund,

### Authorship

Contribution: L.Y.M. and C.M.E. designed the experiments, analyzed the data, prepared figures, and wrote the manuscript; P.J. and Z.Z. analyzed the sequencing data, prepared figures, and assisted in writing the manuscript; K.B.D. assisted in designing the sequencing of patient samples, validating the WGS data, and evaluating data; L.Y.M., D.A.B., R.J.D., and D.H. performed experiments; J.A.Z. provided samples and participated in discussions of the data; J.P.Z. did the pathological evaluation and participated in discussions of the data; U.D. assisted in Figure 5F preparation and participated in data discussions; and all authors reviewed and edited the manuscript.

Conflict-of-interest disclosure: The authors declare no competing financial interests.

Correspondence: Laura Y. McGirt, Levine Cancer Institute 1021 Morehead Medical Dr, Charlotte, NC 28204; e-mail: laura.mcgirt@carolinas.org; and Christine M. Eischen, Department of Pathology,

Microbiology and Immunology, Vanderbilt University Medical Center, Medical Center North CC2210, 1161 21st Ave S, Nashville, TN 37232; e-mail: christine.eischen@vanderbilt.edu.

## References

- Kim YH, Liu HL, Mraz-Gernhard S, Varghese A, Hoppe RT. Long-term outcome of 525 patients with mycosis fungoides and Sezary syndrome: clinical prognostic factors and risk for disease progression. *Arch Dermatol*. 2003;139(7):857-866.
- Jackow CM, Cather JC, Hearne V, Asano AT, Musser JM, Duvic M. Association of erythrodermic cutaneous T-cell lymphoma, superantigen-positive *Staphylococcus aureus*, and oligoclonal T-cell receptor V beta gene expansion. *Blood*. 1997;89(1):32-40.
- Tan RS, Butterworth CM, McLaughlin H, Malka S, Samman PD. Mycosis fungoides—a disease of antigen persistence. *Br J Dermatol*. 1974;91(6):607-616.
- Wohl Y, Tur E. Environmental risk factors for mycosis fungoides. *Curr Probl Dermatol*. 2007;35:52-64.
- McGirt LY, Adams CM, Baerenwald DA, Zwerner JP, Zic JA, Eischen CM. miR-223 regulates cell growth and targets proto-oncogenes in mycosis fungoides/cutaneous T-cell lymphoma. *J Invest Dermatol*. 2014;134(4):1101-1107.
- van Kester MS, Ballabio E, Benner MF, et al. miRNA expression profiling of mycosis fungoides. *Mol Oncol*. 2011;5(3):273-280.
- Whittaker S. Molecular genetics of cutaneous lymphomas. *Ann N Y Acad Sci*. 2001;941:39-45.
- Beyer M, Möbs M, Humme D, Sterry W. Pathogenesis of mycosis fungoides. *J Dtsch Dermatol Ges*. 2011;9(8):594-598.
- Karenko L, Hahtola S, Ranki A. Molecular cytogenetics in the study of cutaneous T-cell lymphomas (CTCL). *Cytogenet Genome Res*. 2007;118(2-4):353-361.
- van Doorn R, van Kester MS, Dijkman R, et al. Oncogenomic analysis of mycosis fungoides reveals major differences with Sezary syndrome. *Blood*. 2009;113(1):127-136.
- Laharanne E, Oumouhou N, Bonnet F, et al. Genome-wide analysis of cutaneous T-cell lymphomas identifies three clinically relevant classes. *J Invest Dermatol*. 2010;130(6):1707-1718.
- Salgado R, Servitje O, Gallardo F, et al. Oligonucleotide array-CGH identifies genomic subgroups and prognostic markers for tumor stage mycosis fungoides. *J Invest Dermatol*. 2010;130(4):1126-1135.
- Abraham RM, Zhang Q, Odum N, Wasik MA. The role of cytokine signaling in the pathogenesis of cutaneous T-cell lymphoma. *Cancer Biol Ther*. 2011;12(12):1019-1022.
- Eriksen KW, Kaltoff K, Mikkelsen G, et al. Constitutive STAT3-activation in Sezary syndrome: tyrostatin AG490 inhibits STAT3-activation, interleukin-2 receptor expression and growth of leukemic Sezary cells. *Leukemia*. 2001;15(5):787-793.
- Fantin VR, Loboda A, Paweletz CP, et al. Constitutive activation of signal transducers and activators of transcription predicts vorinostat resistance in cutaneous T-cell lymphoma. *Cancer Res*. 2008;68(10):3785-3794.
- Koo GC, Tan SY, Tang T, et al. Janus kinase 3-activating mutations identified in natural killer/T-cell lymphoma. *Cancer Discov*. 2012;2(7):591-597.
- Elliott NE, Cleveland SM, Grann V, Janik J, Waldmann TA, Davé UP. FERM domain mutations induce gain of function in JAK3 in adult T-cell leukemia/lymphoma. *Blood*. 2011;118(14):3911-3921.
- Cornejo MG, Kharas MG, Werneck MB, et al. Constitutive JAK3 activation induces lymphoproliferative syndromes in murine bone marrow transplantation models. *Blood*. 2009;113(12):2746-2754.
- Feldman AL, Dogan A, Smith DI, et al. Discovery of recurrent t(6;7)(p25.3;q32.3) translocations in ALK-negative anaplastic large cell lymphomas by massively parallel genomic sequencing. *Blood*. 2011;117(3):915-919.
- Zhang J, Grubor V, Love CL, et al. Genetic heterogeneity of diffuse large B-cell lymphoma. *Proc Natl Acad Sci USA*. 2013;110(4):1398-1403.
- Clark RA, Chong BF, Mirchandani N, et al. A novel method for the isolation of skin resident T cells from normal and diseased human skin. *J Invest Dermatol*. 2006;126(5):1059-1070.
- Li H, Durbin R. Fast and accurate short read alignment with Burrows-Wheeler transform. *Bioinformatics*. 2009;25(14):1754-1760.
- DePristo MA, Banks E, Poplin R, et al. A framework for variation discovery and genotyping using next-generation DNA sequencing data. *Nat Genet*. 2011;43(5):491-498.
- Koboldt DC, Zhang Q, Larson DE, et al. VarScan 2: somatic mutation and copy number alteration discovery in cancer by exome sequencing. *Genome Res*. 2012;22(3):568-576.
- Saunders CT, Wong WS, Swamy S, Becq J, Murray LJ, Cheetham RK. Strelka: accurate somatic small-variant calling from sequenced tumor-normal sample pairs. *Bioinformatics*. 2012;28(14):1811-1817.
- Boeva V, Popova T, Bleakley K, et al. Control-FREEC: a tool for assessing copy number and allelic content using next-generation sequencing data. *Bioinformatics*. 2012;28(3):423-425.
- Boeva V, Zinovyev A, Bleakley K, et al. Control-free calling of copy number alterations in deep-sequencing data using GC-content normalization. *Bioinformatics*. 2011;27(2):268-269.
- Wang J, Mullighan CG, Easton J, et al. CREST maps somatic structural variation in cancer genomes with base-pair resolution. *Nat Methods*. 2011;8(8):652-654.
- Wang K, Li M, Hakonarson H. ANNOVAR: functional annotation of genetic variants from high-throughput sequencing data. *Nucleic Acids Res*. 2010;38(16):e164.
- Li H, Handsaker B, Wysoker A, et al; 1000 Genome Project Data Processing Subgroup. The Sequence Alignment/Map format and SAMtools. *Bioinformatics*. 2009;25(16):2078-2079.
- Jia P, Pao W, Zhao Z. Patterns and processes of somatic mutations in nine major cancers. *BMC Med Genomics*. 2014;7:11.
- Alexandrov LB, Nik-Zainal S, Wedge DC, et al; Australian Pancreatic Cancer Genome Initiative; ICGC Breast Cancer Consortium; ICGC MML-Seq Consortium; ICGC PedBrain. Signatures of mutational processes in human cancer [published correction appears in *Nature*. 2013;502(7470):258]. *Nature*. 2013;500(7463):415-421.
- Alt JR, Greiner TC, Cleveland JL, Eischen CM. Mdm2 haplo-insufficiency profoundly inhibits Myc-induced lymphomagenesis. *EMBO J*. 2003;22(6):1442-1450.
- Lawrence MS, Stojanov P, Polak P, et al. Mutational heterogeneity in cancer and the search for new cancer-associated genes. *Nature*. 2013;499(7457):214-218.
- Mi H, Muruganujan A, Thomas PD. PANTHER in 2013: modeling the evolution of gene function, and other gene attributes, in the context of phylogenetic trees. *Nucleic Acids Res*. 2013;41(Database issue):D377-D386.
- Cancer Cell Line Encyclopedia (CCLE). Comprehensive Cell Line Encyclopedia Version 2.17. Cambridge, MA: The Broad Institute; 2014.
- Zhang C, Richon V, Ni X, Talpur R, Duvic M. Selective induction of apoptosis by histone deacetylase inhibitor SAHA in cutaneous T-cell lymphoma cells: relevance to mechanism of therapeutic action. *J Invest Dermatol*. 2005;125(5):1045-1052.
- Chong BF, Wilson AJ, Gibson HM, et al. Immune function abnormalities in peripheral blood mononuclear cell cytokine expression differentiates stages of cutaneous T-cell lymphoma/mycosis fungoides. *Clin Cancer Res*. 2008;14(3):646-653.
- Yasui DH, Genetta T, Kadesch T, et al. Transcriptional repression of the IL-2 gene in Th cells by ZEB. *J Immunol*. 1998;160(9):4433-4440.
- McGregor JM, Crook T, Fraser-Andrews EA, et al. Spectrum of p53 gene mutations suggests a possible role for ultraviolet radiation in the pathogenesis of advanced cutaneous lymphomas. *J Invest Dermatol*. 1999;112(3):317-321.
- Whibley C, Pharoah PD, Hollstein M. p53 polymorphisms: cancer implications. *Nat Rev Cancer*. 2009;9(2):95-107.
- Mechanic LE, Bowman ED, Welsh JA, et al. Common genetic variation in TP53 is associated with lung cancer risk and prognosis in African Americans and somatic mutations in lung tumors. *Cancer Epidemiol Biomarkers Prev*. 2007;16(2):214-222.
- Sucheston L, Witonsky DB, Hastings D, et al. Natural selection and functional genetic variation in the p53 pathway. *Hum Mol Genet*. 2011;20(8):1502-1508.
- Bray SJ. Notch signalling: a simple pathway becomes complex. *Nat Rev Mol Cell Biol*. 2006;7(9):678-689.
- Pancewicz J, Nicot C. Current views on the role of Notch signaling and the pathogenesis of human leukemia. *BMC Cancer*. 2011;11:502.
- Kiel MJ, Velusamy T, Betz BL, et al. Whole-genome sequencing identifies recurrent somatic NOTCH2 mutations in splenic marginal zone lymphoma. *J Exp Med*. 2012;209(9):1553-1565.
- Witt CM, Hurez V, Swindle CS, Hamada Y, Klug CA. Activated Notch2 potentiates CD8 lineage maturation and promotes the selective development of B1 B cells. *Mol Cell Biol*. 2003;23(23):8637-8650.
- Scott LJ. Tofacitinib: a review of its use in adult patients with rheumatoid arthritis. *Drugs*. 2013;73(8):857-874.
- Krishnaswami S, Chow V, Boy M, Wang C, Chan G. Pharmacokinetics of tofacitinib, a janus kinase inhibitor, in patients with impaired renal function and end-stage renal disease. *J Clin Pharmacol*. 2014;54(1):46-52.
- Huang PH, Chen CH, Chou CC, et al. Histone deacetylase inhibitors stimulate histone H3 lysine 4 methylation in part via transcriptional repression

- of histone H3 lysine 4 demethylases. *Mol Pharmacol*. 2011;79(1):197-206.
51. Mo R, Rao SM, Zhu YJ. Identification of the MLL2 complex as a coactivator for estrogen receptor alpha. *J Biol Chem*. 2006;281(23):15714-15720.
  52. Lohr JG, Stojanov P, Lawrence MS, et al. Discovery and prioritization of somatic mutations in diffuse large B-cell lymphoma (DLBCL) by whole-exome sequencing. *Proc Natl Acad Sci USA*. 2012;109(10):3879-3884.
  53. Wysocka J, Myers MP, Laherty CD, Eisenman RN, Herr W. Human Sin3 deacetylase and trithorax-related Set1/Ash2 histone H3-K4 methyltransferase are tethered together selectively by the cell-proliferation factor HCF-1. *Genes Dev*. 2003;17(7):896-911.
  54. Shema E, Tirosh I, Aylon Y, et al. The histone H2B-specific ubiquitin ligase RNF20/hBRE1 acts as a putative tumor suppressor through selective regulation of gene expression. *Genes Dev*. 2008;22(19):2664-2676.
  55. Kim J, Guermah M, McGinty RK, et al. RAD6-mediated transcription-coupled H2B ubiquitylation directly stimulates H3K4 methylation in human cells. *Cell*. 2009;137(3):459-471.
  56. Mechanic LE, Marrogi AJ, Welsh JA, et al. Polymorphisms in XPD and TP53 and mutation in human lung cancer. *Carcinogenesis*. 2005;26(3):597-604.
  57. Bellei B, Cota C, Amantea A, Muscardin L, Picardo M. Association of p53 Arg72Pro polymorphism and beta-catenin accumulation in mycosis fungoides. *Br J Dermatol*. 2006;155(6):1223-1229.
  58. Klinakis A, Lobry C, Abdel-Wahab O, et al. A novel tumour-suppressor function for the Notch pathway in myeloid leukaemia. *Nature*. 2011;473(7346):230-233.
  59. Lee SY, Kumano K, Nakazaki K, et al. Gain-of-function mutations and copy number increases of Notch2 in diffuse large B-cell lymphoma. *Cancer Sci*. 2009;100(5):920-926.
  60. Fanale D, Iovanna JL, Calvo EL, et al. Analysis of germline gene copy number variants of patients with sporadic pancreatic adenocarcinoma reveals specific variations. *Oncology*. 2013;85(5):306-311.
  61. Krepischi AC, Pearson PL, Rosenberg C. Germline copy number variations and cancer predisposition. *Future Oncol*. 2012;8(4):441-450.
  62. Weng AP, Ferrando AA, Lee W, et al. Activating mutations of NOTCH1 in human T cell acute lymphoblastic leukemia. *Science*. 2004;306(5694):269-271.
  63. Pancewicz J, Taylor JM, Datta A, et al. Notch signaling contributes to proliferation and tumor formation of human T-cell leukemia virus type 1-associated adult T-cell leukemia. *Proc Natl Acad Sci USA*. 2010;107(38):16619-16624.
  64. Kamstrup MR, Biskup E, Gniadecki R. Notch signalling in primary cutaneous CD30+ lymphoproliferative disorders: a new therapeutic approach? *Br J Dermatol*. 2010;163(4):781-788.
  65. Eger A, Aigner K, Sonderegger S, et al. DeltaEF1 is a transcriptional repressor of E-cadherin and regulates epithelial plasticity in breast cancer cells. *Oncogene*. 2005;24(14):2375-2385.
  66. Hidaka T, Nakahata S, Hatakeyama K, et al. Down-regulation of TCF8 is involved in the leukemogenesis of adult T-cell leukemia/lymphoma. *Blood*. 2008;112(2):383-393.
  67. Studniberg HM, Weller P, PUVA, UVB, psoriasis, and nonmelanoma skin cancer. *J Am Acad Dermatol*. 1993;29(6):1013-1022.
  68. Choi DK, Helenowski I, Hijiya N. Secondary malignancies in pediatric cancer survivors: perspectives and review of the literature. *Int J Cancer*. 2014;135(8):1764-1773.